42%-efficient single-pass cw second-harmonic generation in periodically poled lithium niobate

Article *in* Optics Letters · January 1998

DOI: 10.1364/OL.22.001834 · Source: PubMed

42%-efficient single-pass cw second-harmonic generation in periodically poled lithium niobate

G. D. Miller, R. G. Batchko, W. M. Tulloch, D. R. Weise, M. M. Fejer, and R. L. Byer

E. L. Ginzton Laboratory, Stanford University, Stanford, California 94305

Received June 25, 1997

We present a full-wafer fabrication process for periodically poled lithium niobate with a 6.5-μm domain period. Samples that were 53 mm long and 0.5 mm thick were obtained with this process for single-pass cw 1064-nm Nd:YAG second-harmonic generation. These samples exhibited 78% of the ideal nonlinear coefficient, had a measured conversion efficiency of 8.5%/W in the low-power limit, and produced 2.7 W of cw 532-nm output with 6.5 W of cw input, which corresponds to 42% power conversion efficiency. © 1997 Optical Society of America

Since the first demonstration in 1991[1] of the use of electric fields applied through lithographically defined electrodes for patterning of the domain structure of ferroelectrics for quasi-phase-matched interactions, steady progress has been reported. Today quasi-phase-matching (QPM) samples are being widely fabricated with this technique in lithium niobate ($LiNbO_3$),[2–4] $LiTaO_3$, [5,6] and KTP (Ref. 7) and its isomorphs.[8] Recently periodically poled $LiNbO_3$ (PPLN) has become commercially available[9] for parametric interactions in the infrared.

Material dispersion dictates that the period of the domain structure used for QPM must be reduced as the output wavelength is reduced. Infrared interactions in $LiNbO_3$ typically require samples with domain periods of 15–30 μm, whereas visible interactions generally require domain periods of 2–15 μm. As the period is decreased to less than 10 μm, interactions between domains during poling result in large variations in the domain duty cycle, limiting the length and overall conversion efficiency of visible light samples.[10] Although infrared samples can be fabricated on a wafer scale[11] with lengths as great as 50 mm, visible light samples have been limited to lengths of 10 mm owing to issues of domain pattern quality.

In this Letter we present a method for fabricating full wafers of PPLN with a 6.5-μm domain period; we than present the results of second-harmonic-generation (SHG) experiments performed with samples made with this method. These samples were 53 mm long and 0.5 mm thick and were used for single-pass cw 1064-nm Nd:YAG SHG. The 6.5-μm domain period was chosen for phase matching at $\sim$200 °C for suppression of residual photorefractive damage.[12] The effective nonlinear coefficient of the samples was 78% of ideal [$d_{\text{eff}} = 0.78(2/\pi)d_{33}$], resulting in a measured power efficiency of 8.5%/W for confocal[13] focusing. Experimentally we demonstrated 2.7 W cw of 532-nm harmonic output at 42% efficiency.

We focused on understanding the domain formation process in $LiNbO_3$ to improve domain pattern quality for visible light samples. A strong relationship exists between the electric field in the substrate during poling and the rate at which domains grow in a direction parallel to the **k** vector of the electrode grating. As these domains spread beyond the electrodes and under an insulator, an unscreened spontaneous polarization charge is deposited upon the surface of the substrate. This charge lowers the average field in the substrate, slowing the transverse growth of the domains. Domain growth can be made to be self-limiting by selection of an optimum poling field strength of 20.75 kV/mm, the field at which the domain growth rate is most sensitive to changes in the average substrate field. In addition, the density of domain nucleation sites must be increased as the domain period is reduced for uniform domain pattern quality. Reference 14 provides further details on this model of electric-field poling. The combination of optimum poling fields with sufficiently high nucleation site density allowed us to fabricate uniform samples on a wafer scale.

The processing steps for obtaining 6.5-μm-period PPLN on a wafer scale are described next. The $+z$ face of an optical-grade z-cut $LiNbO_3$ wafer was lithographically patterned with a periodic array of sputtered nichrome stripes with the grating **k** vector parallel to the crystallographic x axis. The wafers, made by Crystal Technology, Inc., had a 500-μm nominal thickness and a 76.2-mm diameter. The nichrome composition was 80% Ni, 20% Cr. The nichrome stripes were 50 nm thick, 1 μm wide, 60 mm long, and had a period of 6.5 μm. With 1-μm-wide stripes, the electric-field poling model[14] predicts a domain duty cycle of 35%. Although a 50% domain duty cycle is preferable, the lower duty cycle was chosen for reduction of the merging of domains. The metallized $+z$ face was overcoated with a 0.5-μm-thick spin-on-glass (Allied Signal) insulator cured at 350 °C in air for 8 h. An annular electrolyte-contact window, 55 mm in diameter and 2 mm wide, was opened in the insulator with hydrofluoric acid and a photoresist mask. We added two additional contact windows to compensate for discontinuous metal stripes caused by defects in lithography. Next the thickness of the wafer was measured for use in determining the voltage required for the desired poling field. The wafer was then loaded into an electrolyte-contacting fixture of a type previously reported.[15] The electrolyte used

0146-9592/97/241834-03$10.00/0

was a saturated solution of lithium chloride in water. The electrolyte contacted the $-z$ face uniformly. On the $+z$ face the electrolyte contacted the insulator uniformly and the metal stripes were contacted by the electrolyte through the electrolyte-contact windows.

The assembled fixture was connected to a Trek Model 20/20 high-voltage amplifier driven by a SRS DS345 arbitrary waveform generator. The Trek is a voltage-regulated high-voltage amplifier with a nominal current limit of 20 mA. The voltage across the contact fixture was recorded by the amplifier's voltage monitor output and a LeCroy 9304M oscilloscope. The current through the wafer was monitored with a 1-kΩ series resistor to ground. The waveform generator was programmed to apply 21.5 kV/mm to the wafer to maximize domain nucleation site density.[14] When the poling current increased to the amplifier's current limit, the applied field decreased to 20.9 kV/mm. We delivered the pulse for 140 ms to pole the material, stepped the pulse to 19.5 kV/mm for 10 ms, and then ramped it to 0 kV/mm over 60 ms to prevent the spontaneous erasure of domains.[14] The wafer was removed from the fixture, the insulator and metal were etched away, and the wafer was etched in hydrofluoric acid to reveal the overall uniformity of the domain pattern. This procedure was repeated for a second wafer. Both wafers showed good domain pattern uniformity. We polished and then etched in hydrofluoric acid the y face of a sample taken from one of these wafers to reveal the domain quality through the volume of the material. Figure 1 shows the etched y face through the 0.5-mm-thick sample. Close visual inspection shows good domain uniformity with a duty cycle close to the 35% predicted by the model. Approximately 5% of the domains merged at depths of 100 to 150 μm.

Seven 53-mm-long, 3-mm-wide samples were cut from the two wafers. For characterization by SHG the sample endfaces were polished but left uncoated. The TEM_{00} output of a Lightwave Series 122 single-frequency Nd:YAG laser was loosely focused through several of the samples for determination of their phase-matching characteristics and effective nonlinear coefficients. Figure 2 shows a SHG temperature-tuning curve for one of these samples. The observed phase-matching temperature was 199.5 °C, which compares favorably with a predicted phase-matching temperature of 195.6 °C that was determined with a recently published temperature-dependent Sellmeier equation for $LiNbO_3$ (Ref. 16) and with thermal expansion taken into account. The theoretical phase-matching curve for a 53-mm-long sample was shifted in temperature in Fig. 2 for comparison with the 199.5 °C experimental phase-matching data. The excellent agreement indicates that domain periodicity, the material dispersion, and the oven temperature profile were uniform over the entire 53-mm-sample length. Using measurements of conversion efficiency in the loose-focus low-power limit, beam dimensions, and crystal length, we calculated the effective nonlinear coefficient to be 14 pm/V, 78% of the value for an ideal first-order QPM grating and 88% of the 16 pm/V expected for a uniform 35% duty cycle. Both the predicted and the measured single-pass conversion efficiencies for confocally focused interactions were 8.5%, as opposed to the 14%/W predicted for perfect first-order QPM.

We next tested these samples at higher power levels by single-pass cw SHG with an 8-W cw Lightwave Series 220 Nd:YAG laser ($M^2 \approx 1.3$). During these measurements, absorption by the fundamental and the harmonic beams gave rise to thermal lensing and apparent shifts in the phase-matching temperature. To compensate for these effects, we adjusted the input beam-waist size and location and the oven temperature for each value of input fundamental power to maximize harmonic output power. Figure 3 shows the generated 532-nm output power versus 1064-nm input power for one sample in which second-harmonic output power was maximized for each value of fundamental input power. All powers are internal to the sample and corrected for Fresnel reflection at the endfaces.

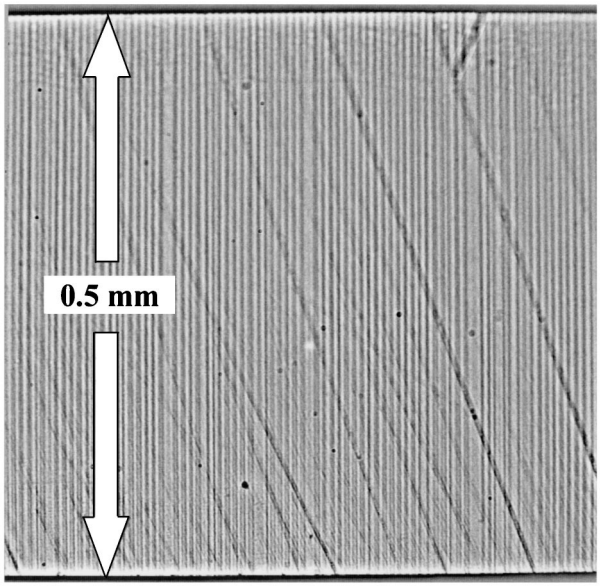

Fig. 1. Etched y face of 0.5-mm-thick periodically poled $LiNbO_3$ showing 6.5-μm period domains. The domain duty cycle is approximately 35%. The diagonal features are polishing scratches.

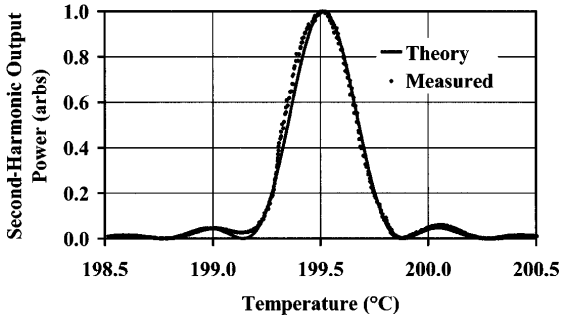

Fig. 2. 532-nm output power [in arbitrary units (arbs)] versus temperature for Nd:YAG SHG. The dots are experimental data, and the solid curve is the theoretical plane-wave curve for a 53-mm sample, shifted to the same peak phase-matching temperature. The good agreement between data and theory indicates the sample phase matches over the full 53-mm length.

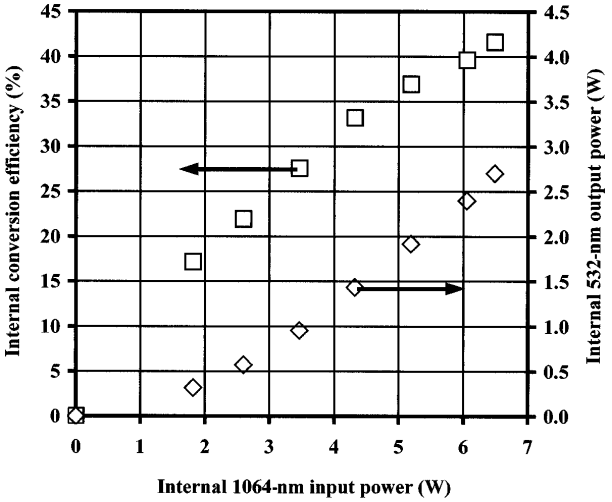

Fig. 3. Measured cw 532-nm output power internal to the exit face of the sample versus 1064-nm input power internal to the input face of the sample. The conversion efficiency for cw single-pass Nd:YAG SHG was 42% at 6.5 W of input power, yielding 2.7 W of 532-nm output power.

Second-harmonic power of 2.7 W was generated for 6.5 W of input; the internal conversion efficiency was 42%. This conversion efficiency is more than an order of magnitude greater than that previously obtained[17] for cw single-pass SHG in a bulk material.

For 1064-nm input powers exceeding ~3 W, both the 532- and the 1064-nm output beams exhibited pointing instability when the temperature was tuned to phase matching. The instability was transient, decaying in less than 1 h. The pointing instability was anisotropic, and the beam deviated parallel to the crystalline z axis. The anisotropic nature of this instability is suggestive of photorefractive damage. Further investigation is required for better understanding of this behavior.

For 1064-nm input powers exceeding ~5.5 W, both the 532- and the 1064-nm output beams exhibited spot-size instability when the temperature was tuned to phase matching. The fundamental output beam did not exhibit this instability when the temperature was tuned away from phase matching. The presence of a significant amount of second harmonic, with its higher absorption coefficient, can be expected to give rise to increased thermal self-focusing, which can in turn cause spot-size instabilities and eventually filament formation. With a fundamental input power of 6.5 W, the sample whose data are shown in Fig. 3 operated for approximately 1 h before damage occurred as a result of the formation of a beam filament. We expect in the future that lowering $LiNbO_3$'s absorption coefficient in the visible, for example, through careful postgrowth processing for control of its oxidation and stoichiometry, will lead to improved performance and increased 532-nm output power.

In conclusion, we have presented a method for fabricating full wafers of PPLN with a 6.5-μm domain period for SHG of 532-nm radiation. We have shown that material produced with this method was phase matched over a 53-mm length, had an 8.5%/W single-pass conversion efficiency in the low-power limit, and produced 2.7 W of cw 532-nm output with 42% single-pass efficiency.

This research was sponsored by the Defense Advanced Research Projects Agency/U.S. Office of Naval Research (ONR) through the Center for Nonlinear Optical Materials at Stanford University under ONR grant N00014-92-J-1903. We thank Larry Myers and Wright–Patterson Air Force Base for the use of the Lightwave Series 220 laser. G. Miller thanks General Motors for tuition and salary support through the General Motors Fellowship Plan.

References

1. S. Matsumoto, E. J. Lim, H. M. Hertz, and M. M. Fejer, Electron. Lett. **27,** 2040 (1991).
2. M. Yamada, N. Nada, M. Saitoh, and K. Watanabe, Appl. Phys. Lett. **62,** 435 (1993).
3. J. Webjorn, V. Pruneri, P. St. J. Russell, J. R. M. Barr, and D. C. Hanna, Electron. Lett. **30,** 894 (1994).
4. L. E. Myers, G. D. Miller, R. C. Eckardt, M. M. Fejer, and R. L. Byer, Opt. Lett. **20,** 52 (1995).
5. S. Zhu, Y. Zhu, Z. Zhang, H. Shuu, H. Wang, J. Hong, C. Ge, and N. Ming, J. Appl. Phys. **77,** 5481 (1995).
6. K. Mizuuchi and K. Yamamoto, Appl. Phys. Lett. **66,** 2943 (1995).
7. Q. Chen and W. P. Risk, Electron. Lett. **30,** 1516 (1994).
8. W. P. Risk and G. M. Loiacono, Appl. Phys. Lett. **69,** 311 (1996).
9. Crystal Technology and Deacon Research, both of Palo Alto, California.
10. M. M. Fejer, G. A. Magel, D. H. Jundt, and R. L. Byer, IEEE J. Quantum Electron. **28,** 2631 (1992).
11. L. E. Myers, W. R. Bosenberg, J. L. Alexander, M. A. Arbore, M. M. Fejer, and R. L. Byer, in *Advanced Solid-State Lasers*, S. A. Payne and C. R. Pollock, eds., Vol. 1 of Trends in Optics and Photonics Series (Optical Society of America, Washington, D.C., 1996), p. 35.
12. M. Taya, M. C. Bashaw, and M. M. Fejer, Opt. Lett. **21,** 857 (1996).
13. A. Yariv and P. Yeh, in *Optical Waves in Crystals* (Wiley, New York, 1984), p. 530.
14. G. D. Miller, R. G. Batchko, M. M. Fejer, and R. L. Byer, Proc. SPIE **2700,** 34 (1996).
15. L. E. Myers, R. C. Eckardt, M. M. Fejer, R. L. Byer, W. R. Bosenberg, and J. W. Pierce, J. Opt. Soc. Am. B **12,** 2102 (1995).
16. D. H. Jundt, Opt. Lett. **22,** 1553 (1997).
17. T. Pliska, D. Fluck, and P. Guenter, Helv. Phys. Acta **68,** 502 (1995).